DOI: 10.1021/cg900874f

CRYSTAL GROWTH & DESIGN Article
2010, Vol. 10
244–251

A Network of Small Molecules Connected by Cross-Linked NH Bonds

Gaetano Angelici,[†] Nicola Castellucci,[†] Simone Contaldi,[†] Giuseppe Falini,[†] Hans-Jörg Hofmann,[‡] Magda Monari,*[,†] and Claudia Tomasini*[,†]

[†]*Dipartimento di Chimica "G. Ciamician", Alma Mater Studiorum Università di Bologna - Via Selmi 2, I-40126 Bologna, Italy, and* [‡]*Institute of Biochemistry, University of Leipzig - Brüderstrasse 34, D-04103 Leipzig, Germany*

Received July 27, 2009; Revised Manuscript Received September 14, 2009

ABSTRACT: The synthesis of the small pseudopeptide Boc-L-Phe-D-Imz-OBn (Imz = imidazolidin-2-one-4-carboxylate) is reported. Crystallization of this peptide from methanol, ethanol, and isopropanol leads to isostructural solvates when the solvent is methanol or ethanol with a peptide/solvent ratio of 2:1 and to an unsolvated polymorph in the case of isopropanol. The solvate peptide crystallizes forming infinite chains with the monomers in parallel orientation connected by a single hydrogen bond. The chains are arranged in antiparallel direction and cross-linked through the NH group of the imidazolidin heterocycle with formation of a stable two-dimensional (2D) network. Crystals from isopropanol form a different 2D network. The degree of order in the crystal assembly decreases from methanol and ethanol solvates to the unsolvated pseudopeptide grown from isopropanol. Quantum chemical calculations at the HF/6-31G* level of ab initio MO theory, carried out on the two different packings, show a slight preference for the unsolvated packing.

Introduction

Synthetic oligomers which are able to form stable secondary structures have been defined as "foldamers".[1] Foldamer research was essentially stimulated by the investigation of peptidic foldamers composed of unnatural and proteinogenic amino acids or even completely of unnatural amino acids.[2] These molecules are designed and prepared with the aim of forming three-dimensional structures that mimic complex natural structures, such as peptides and proteins. Sometimes, these compounds exhibit interesting novel properties, as for instance antibacterial or anticancer effects.[3] Furthermore, they might be applied against neurodegenerative diseases that are characterized by the formation of amyloidal peptides, resulting from the degradation of natural proteins.[4] Therefore, the study of foldamers, in particular representatives with potential biological activity, is highly desirable.

Recently, it was shown[5] that there is no need of very long molecules to form fiber-like materials. Formation of fibrils might even be prevented in longer molecules by the formation of intramolecular hydrogen bonds instead of the required intermolecular interactions. In contrast, small molecules could be good candidates to form fiber- and fibril-like materials, provided that they are rigid enough to assume well-defined conformations. The formation of unconventional "polymers",[6] where the chains are not only formed by covalent bonds, but also by weaker interactions, such as hydrogen bonds, electrostatic interactions, π-stacking interactions, and noncovalent interactions, is possible. If all these weaker interactions cooperate, the formation of peptide-based nanomaterials can be observed.

We have recently described the formation of a fiber-like material obtained by the slow evaporation of a solution of the dipeptide Boc-L-Phe-D-Oxd-OBn (Boc = tert-butoxycarbonyl; Phe = phenylalanine; Oxd = 4-methyl-5-carboxy oxazolidin-2-one; Bn = benzyl) in a 1:1 mixture of cyclohexane/ethyl acetate.[7] This compound forms fibers with the monomers arranged in infinite chains connected only by a single hydrogen bond.[8] It may be tempting to look for other molecules with such unusual properties. Thus, we synthesized the pseudodipeptide Boc-L-Phe-D-Imz-OBn **1** (Imz = imidazolidin-2-one-4-carboxylate) and investigated its structure in the solid state. This compound is similar to Boc-L-Phe-D-Oxd-OBn but contains an additional NH group in the heterocyclic ring oriented nearly orthogonal to the pre-existing one (Figure 1). The presence of two NH hydrogen bonds that are not oriented along the same axis should favor the formation of a two-dimensional arrangement. This effect should drive the formation of layers instead of fibers, that were obtained with Boc-L-Phe-D-Oxd-OBn, which can form only one hydrogen bond.

Experimental Section

Synthesis. The melting points of the compounds were determined in open capillaries and are not precise (see Thermal Analyses). High quality infrared spectra (64 scans) were obtained at 2 cm^{-1} resolution using a 1 mm NaCl solution cell and a Nicolet 210 FT-infrared spectrometer. The spectra were obtained in 3 mM solutions in dry CH_2Cl_2 at 297 K or as a 1% mixture in dry KBr. All compounds were dried in a vacuum, and all the sample preparations were performed in a nitrogen atmosphere. NMR spectra were recorded with spectrometers at 400 MHz (^{1}H NMR) and at 100 MHz (^{13}C NMR). The proton signals were assigned by gCOSY spectra. Chemical shifts are reported in δ values relative to the solvent peak. Boc-L-Phe-D-Asn-OBn was prepared by coupling of Boc-L-Phe-OH and H-Asn-OBn in solution utilizing conventional methods.

Boc-L-Phe-D-Imz-OBn 1. DBU (0.127 mL, 0.85 mmol) was added to a stirred solution of Boc-L-Phe-D-Asn-OBn (0.2 g, 0.43 mmol) in THF (20 mL). The mixture was stirred for 10 min. Then, $PhI(OAc)_2$ (274 mg, 0.85 mmol) was added and the mixture was stirred at room temperature for 45 min. After this time, a few drops (< 1 mL) of H_2O were added, and the mixture was stirred for another 15 min. The reaction mixture was gently concentrated. The resulting yellow liquid was dissolved in ethyl acetate and washed with H_2O, dried over Na_2SO_4, filtered, concentrated, and dried under a vacuum. The crude was purified by flash chromatography (cyclohexane/ethyl

*To whom correspondence should be addressed. E-mail: claudia.tomasini@unibo.it (C.T.), magda.monari@unibo.it (M.M.).

 Published on Web 10/05/2009

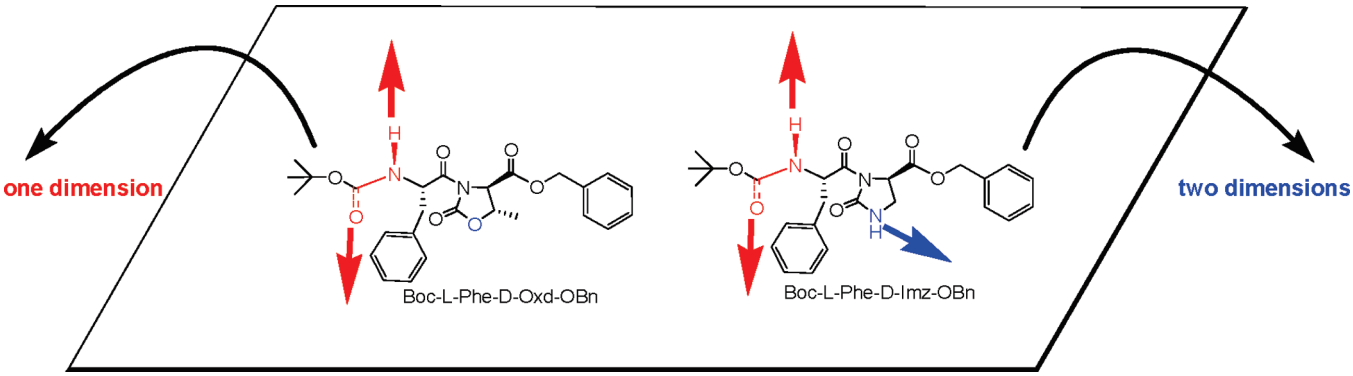

Figure 1. Schematic structural comparison of Boc-L-Phe-D-Oxd-OBn and Boc-L-Phe-D-Imz-OBn (red and blue arrows show the hydrogen bond directions).

acetate 1:1 as eluant) and **1** was obtained pure in 65% yield. Mp = 68 °C; $[\alpha]_D$ +0.081 (c 1.0, CH_2Cl_2); IR (CH_2Cl_2, 10 mM): ν = 3444, 1759, 1716, 1689 cm^{-1}; IR (1% in dry KBr): ν = 3391, 1761, 1687 cm^{-1}; ^1H NMR ($CDCl_3$, 300 MHz): δ 1.42 (s, 9H, *t*-Bu), 2.95 (dd, 1H, J = 7.5, 13.8 Hz, CHN−CH*H*-Ph), 3.2 (dd, 1H, J = 4.8, 13.5 Hz, CHN-C*H*H-Ph), 3.4 (dd, 1H, J = 3.0, 9.3 Hz, NCH*H*), 3.7 (t, 1H, J = 9.9 Hz, NC*H*), 4.8 (m, 1H, NC*H*H), 5.2−5.4 (m, 3H, OCH_2Ph + Boc-N*H*), 5.85 (bs, 1H, N*H*), 5.95 (m, 1H, C*H*N-CHH-Ph), 7.2−7.4 (m, 10H, 2 × Ph); ^{13}C NMR ($CDCl_3$, 75 MHz): δ 28.5, 39.9, 40.6, 54.1, 55.4, 68.0, 127.0, 128.6, 129.0, 129.9, 135.2, 136.6, 154.7, 155.0, 169.1, 172.7.

Plate-Like Crystal Precipitation. The purified compound was crystallized by slow evaporation of a solution of **1** (35 mg) in methanol, ethanol, or isopropanol (1 mL in each case). Crystals called **1a** (crystallized from methanol), **1b** (crystallized from ethanol), and **1c** (crystallized from isopropanol) were prepared.

Imaging. The solid material was observed by optical microscopy (OM) and scanning electron microscopy (SEM). The OM images were collected using a Leica optical microscope equipped with a CCD camera. Samples SEM images were collected on glass coverslip after coating with gold and observed using Philips 515 SEM. The images were recorded using a CCD digital camera.

Single Crystal X-ray Diffraction for 1a, 1b, and 1c. The X-ray intensity data for **1a**, **1b**, and **1c** were measured on a Bruker SMART Apex II CCD area detector diffractometer. Cell dimensions and the orientation matrix were initially determined from a least-squares refinement on reflections measured in three sets of 20 exposures, collected in three different ω regions, and eventually refined against all data. A full sphere of reciprocal space was scanned by 0.3° ω steps. The software SMART[9] was used for collecting frames of data, indexing reflections, and determination of lattice parameters. The collected frames were then processed for integration by the SAINT program,[10] and an empirical absorption correction was applied using SADABS.[11] The structures were solved by direct methods (SIR 97)[11] and subsequent Fourier analysis and refined by full-matrix least-squares on F^2 (SHELXTL),[12] using anisotropic thermal parameters for all non-hydrogen atoms. All hydrogen atoms, except the N−H protons and methine hydrogens, were added in calculated positions, included in the final stage of refinement with isotropic thermal parameters, U(H) = 1.2U_{eq}(C)[U(H) = 1.5U_{eq}(C-Me)], and allowed to ride on their carrier atoms. The absolute structure configuration was not determined from X-ray data but was known from the synthetic route. Crystal data and experimental details for **1a, 1b**, and **1c** are reported in Table S1, Supporting Information.

X-ray Powder Diffraction Analysis. Powder X-ray diffraction patterns were collected using a PanAnalytical X'Pert Pro equipped with X'Celerator detector powder diffractometer using Cu Kα radiation generated at 40 kV and 40 mA. The instrument was configured with a 1/32° divergence and 1/32° antiscattering slits. A standard quartz sample holder 1 mm deep, 20 mm high, and 15 mm wide was used. The diffraction patterns were collected within the 2θ range from 3° to 40° with a step size (Δ 2θ) of 0.02° and a counting time of 300 s.

Thermal Analysis. Calorimetric measurements were performed using a Perkin-Elmer DSC-7. Temperature and enthalpy calibrations were performed by using high purity standards (*n*-decane, benzene, and indium). The material (about 1.5 mg of sample) was sealed in aluminum pans. Heating was carried out at 3 °C min^{-1} in the temperature range 20−200 °C. Transition, denaturation, or desolvation temperatures (TD) were determined as the maximum peak value of the corresponding endothermic phenomena. Weight loss during heating was evaluated by thermogravimetric analysis (TGA) using a calorimeter DSC-Q100 from TA Instruments Waters (USA). The temperature range was from 23 to 350 °C at a heating rate of 5 °C/min under dry nitrogen atmosphere.

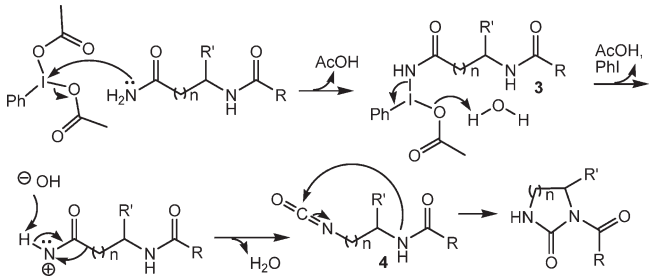

Figure 2. Suggested mechanism of the modified Hofmann rearrangement for the synthesis of 4-substituted imidazolidin-2-one.

Calculations. A detailed conformational analysis of Boc-L-Phe-D-Imz-OBn and calculations on the various crystal packages were performed at the HF/6-31G* level of ab initio MO theory. The Gaussian03 software package was employed in all cases.[13] The details are given in the Supporting Information.

Results and Discussion

The dipeptide Boc-L-Phe-D-Imz-OBn **1** was prepared in a single step starting from the readily available Boc-L-Phe-D-Asn-OBn (Asn = asparagine) utilizing a modified methodology for the Hofmann rearrangement that we have recently described.[14] This method was necessary because the preparation of an imidazolidin-2-one-4-carboxylate could not be performed by reaction of 1,2-diaminopropanoic acid (DAP) with triphosgene, due to the low availability of DAP and the poor reaction yield.

The rearrangement is a very general reaction and can be applied both to protected asparagine and to asparagine-containing protected polypeptides. It is promoted by the readily available $PhI(OAc)_2$ in the presence of DBU (DBU = 1,8-diazabicyclo[5,4,0]undec-7-ene) and provides the desired heterocycle in high yield (Figure 2).

After preparation and purification with conventional methods, Boc-L-Phe-D-Asn-OBn was treated with $PhI(OAc)_2$ and DBU in tetrahydrofuran for 1 h to furnish the desired compound **1** in 65% yield after flash chromatography (Scheme 1).

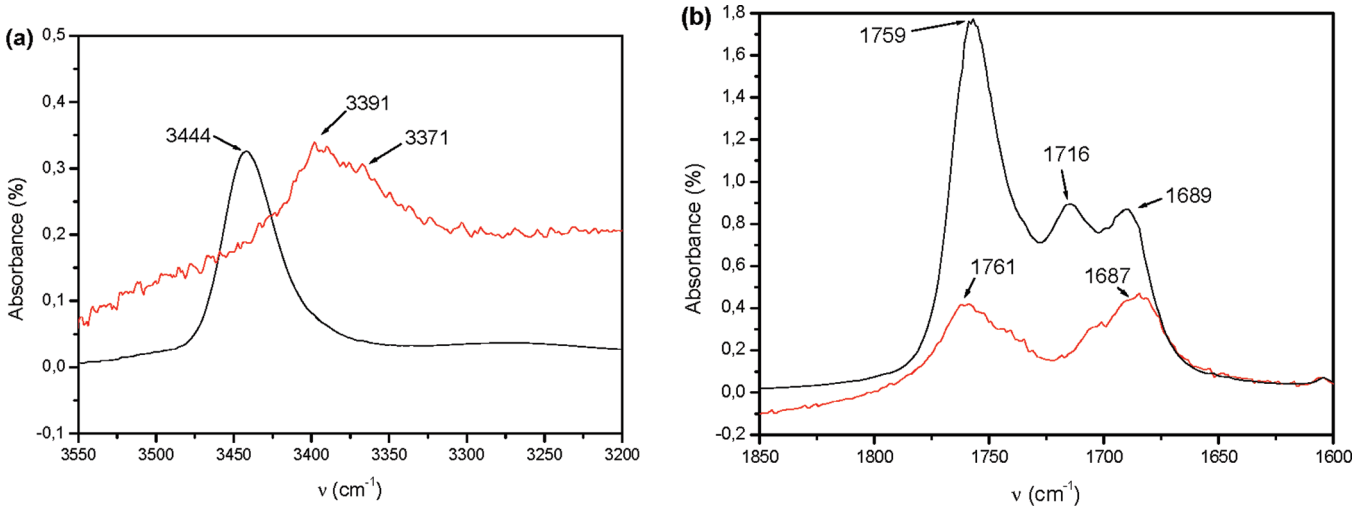

Figure 3. FT-IR absorption spectra (a) in the N−H stretching region (3600−3200 cm^{-1}) and (b) in the C=O stretching region (1850−1600 cm^{-1}) for 3 mM samples of **1** in pure CH_2Cl_2 (black line) and as a 1% solid mixture with KBr (red line) at room temperature.

Scheme 1. Synthesis of Boc-L-Phe-D-Imz-OBn 1

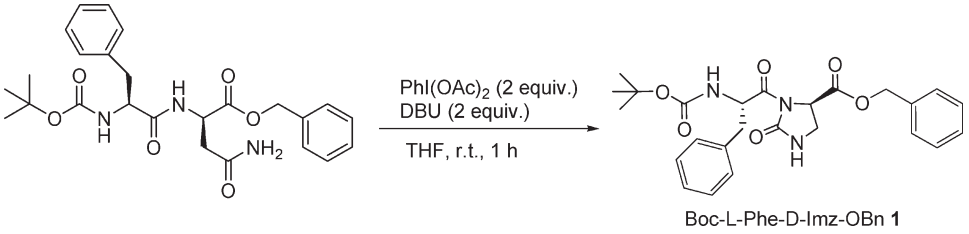

The conformation of compound **1** was analyzed in solution and in the solid state. A first analysis was performed, comparing the IR spectrum of a 3 mM solution of **1** in dichloromethane with the spectrum of a 1% mixture of **1** in KBr. The spectral regions concerning the NH and CO stretching bands are reported in Figure 3.

While hydrogen bonding is clearly present in the solid state as shown by two peaks (3391 and 3371 cm^{-1}) belonging to a broadband, no hydrogen bonding is present in the diluted solution (3444 cm^{-1}), and thus intramolecular NH hydrogen bonds are absent. A strong variation of the spectrum in the CO region confirms this result.

Several attempts were made to obtain macroscopic ordered structures in the solid state by slow evaporation of solutions of **1** in different solvents. The formation of crystal aggregates of **1** was observed by slow evaporation of a 1:1 mixture of cyclohexane/ethyl acetate, which was used for the evaporation of Boc-L-Phe-D-Oxd-OBn. This material was highly crystalline, as shown by the powder X-ray diffraction pattern (Figure S3, Supporting Information).

In contrast, slow evaporation from protonated solvents such as methanol, ethanol, and isopropanol provided crystals, which were useful for single crystal X-ray diffraction studies. Interestingly, the nature of the alcohol has an influence on the preferential elongation and macroscopic side-aggregation of the crystals (Figure 4), which show a common tendency to aggregate laterally along their main axis (Figure 4a,c,e). In the aggregates of **1a**, the lateral association extends over several hundred micrometers. Their image under the optical microscope with cross polars shows them preferentially iso-oriented (insets in Figure 4a). The degree of order in crystal association continuously decreased when ethanol and isopropanol were used as solvents, as shown by the reduced birefringence of crystals **1b** and **1c** (insets in Figure 4c,e). A mismatch in lateral aggregation is present in **1b** (insets in Figure 4d) and becomes remarkable in **1c**, where the crystals show a low birefringence (inset in Figure 4e). However, all these aggregates are highly crystalline, as shown by the X-ray diffraction pattern (Figure S3, Supporting Information). Crystals suitable for single crystal X-ray diffraction were obtained from isopropanol solutions in a crystallization trial using seed crystals from the homogeneous precipitation in the same solvent (Figure 4f). This material is the same polymorph of that obtained from homogeneous precipitation from isopropanol (Figure S3, Supporting Information). The observation of crystals by SEM (Figure 4b,d,f) shows that each crystal is made of several layers which are cast on the top of each other. This superstructure organization is also present in the single crystals obtained from isopropanol by seeding (inset of Figure 4f). Thus, in all these crystals a plywood structure is present, with a varying degree of order as a function of the precipitation conditions.

The formation of these plate-like crystals only by slow evaporation of the protonated solvents suggests the idea that the solvents may play an active role in crystal formation.[8] The obtained single crystals were analyzed by X-ray diffraction (XRD) and thermal analysis. Crystals of **1** grown from methanol and ethanol, respectively, show the formation of methanol (**1a**) and ethanol solvates (**1b**). In addition to the solvent, two independent molecules of **1** are present in the unit cell (Figure 5).

The two peptide molecules in structure **1a** have approximately the same backbone conformation (Table 1, Figure 5). The two conformers differ only in the orientation of the benzyl

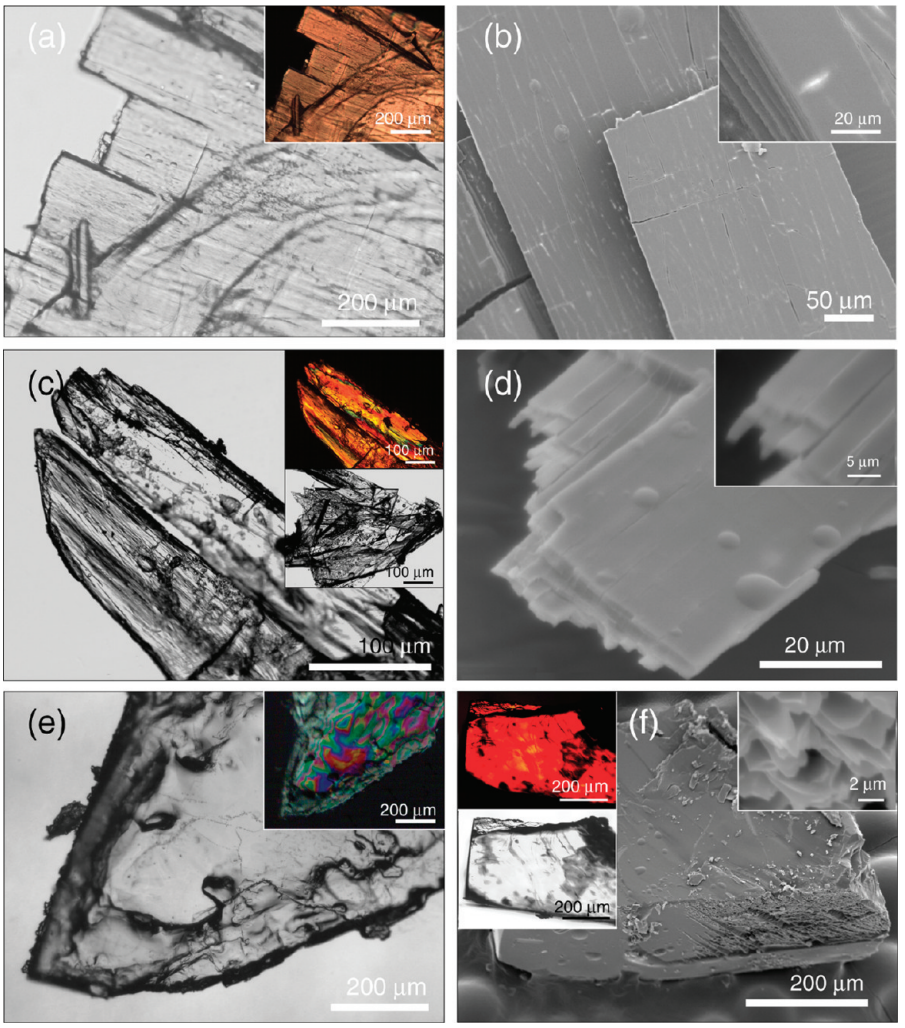

Figure 4. Optical micrographs of crystals of **1** precipitated by slow evaporation from solutions of **1** in (a) **1a** from methanol, (c) **1b** from ethanol, and (e) **1c** from isopropanol. The top insets in (a, c, e) show the same images under cross polars. The bottom inset (c) shows an aggregate of plate-like crystals precipitated from an ethanol solution. In the left insets in (f) optical micrographs of a crystal of **1c** are shown obtained in a seeding crystallization trial from an isopropanol solution. Scanning electron microscopy images of crystals of **1a**, **1b**, and **1c** are shown in (b), (d), and (f), respectively. The plywood structure is evident for **1a** (b) and **1b** (d). The insets in (b) and (d), and that on the right in (f), show that all crystals are made of several layers.

ring of the OBn moiety (see the superimposition in Figure S4, Supporting Information). In the unit cell, each conformer belongs to a separate infinite chain of peptide molecules, which are arranged in parallel orientation. Two consecutive residues in the chains are connected by only one NH···O=C hydrogen bond between the amidic NH proton of the L-Phe residue of the one peptide molecule and the carbonyl function of the *t*-Boc group of the other one (Table 2).

The infinite chains are arranged in an antiparallel orientation along the *a* axis (Figure 6a). The phenyl rings are in a displaced stacked arrangement, but the offset of the phenyls prevents $\pi-\pi$ stacking. The conformation of the monomers and the arrangement of the chains is in close correspondence to that found in Boc-L-Phe-D-Oxd-OBn.[7] However, the backbone torsion angle ψ of the D-Imz constituents is $-163.2°$ and $-150.8°$, respectively, different from that in D-Oxd, which is 23.4°. According to the quantum chemical calculations, these two conformers can be realized both in D-Oxd and in D-Imz. They are the most stable conformers and close together in energy (see Supporting Information). The presence of the NH unit in D-Imz, replacing the oxygen atom in the D-Oxd ring, allows the formation of further hydrogen bonds. This possibility leads to an interconnection of two peptide chains via the bifurcated NH bond involving the Imz NH group of a peptide molecule of one chain and two carbonyls of the other chain. One carbonyl group comes from an L-Phe residue, and the other from the D-Imz constituent of the other chain. Although the NH···OC distances are larger (2.35 and 2.52 Å) than those found in typical hydrogen bonds, the general electrostatic effect in this arrangement favors the interconnection. In comparison to the D-Oxd crystals, the packing is more complex because of the presence of one methanol molecule that acts as a linker between the two chains establishing two H-bonds using both the oxygen and hydrogen atoms (O13−H80···O8, O13···H1−N1) of the solvent molecule (Figure 6b).

As a result of these interchain interactions involving also the methanol molecule, the solid-state arrangement of **1a** can be described as a 2D network made of layers, which are parallel to the *ab* plane (Figure 6a).

The single crystal X-ray diffraction study carried out on crystals of **1** grown from ethanol shows the formation of an ethanol solvate **1b** (Tables S2 and S3, Supporting Information, Figure 5b) isostructural with the methanol solvate **1a**.

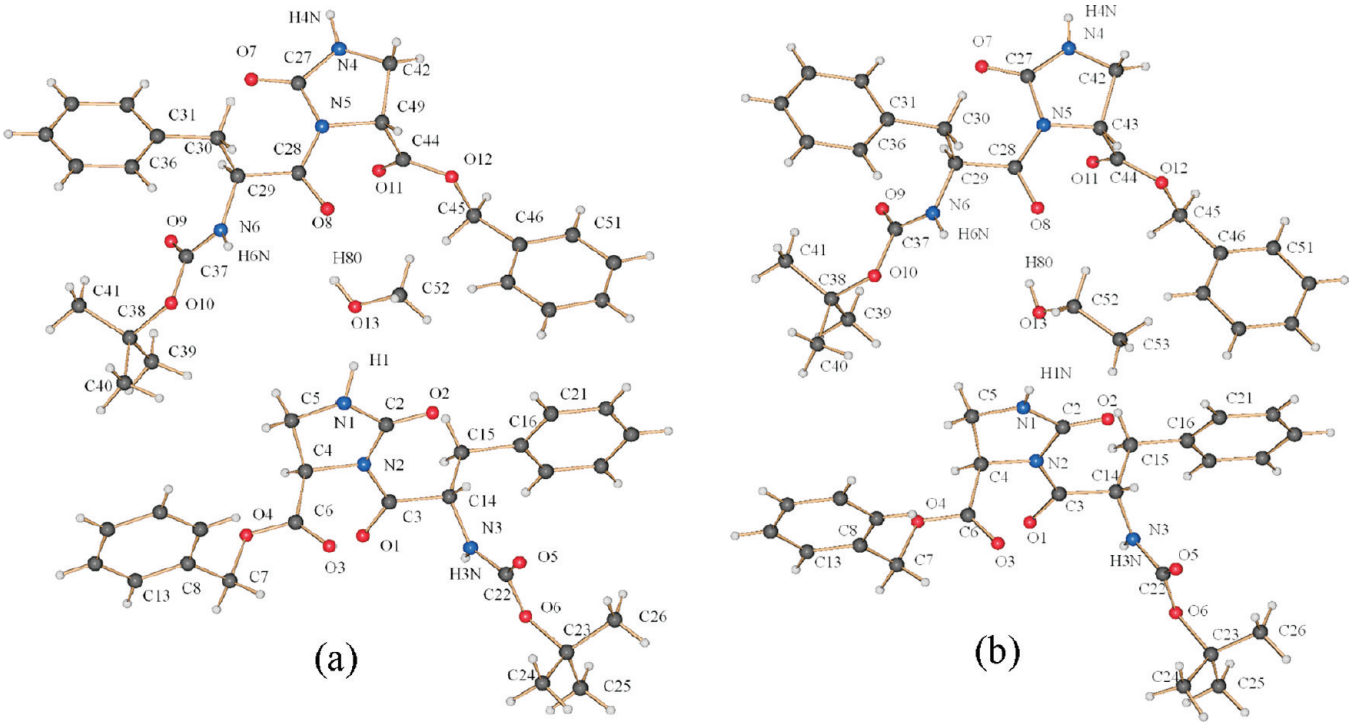

Figure 5. View of the content of the unit cell of **1** crystallized with (a) methanol (structure **1a**) and (b) ethanol (structure **1b**).

Table 1. Comparison of the Backbone Torsion Angles for the Two Independent Molecules of 1a (Methanol Solvate)

torsion angles[a]	molecule A	molecule B
C22−N3−C14−C3 (ϕ1)	−116.9(4)	
N3−C14−C3−N2 (ψ1)	159.7(4)	
N2−C4−C6−O4 (ϕ2)	163.2(5)	
C37−N6−C29−C28 (ϕ1)		−124.8(4)
N6−C29−C28−N5 (ψ1)		169.6(4)
N5−C43−C44−O12 (ϕ2)		−150.8(4)

[a] For atom numbering, see Figure 5.

Table 2. Hydrogen Bond Parameters for 1a[a]

D−H···A	H···A[b]	D···A[b]	∠D−H···A[c]
N3−H3N···O5$^{(1)}$	2.232	3.058(5)	164.19
N1−H1···O13	1.879	2.788(7)	152.87
N6−H6N···O9$^{(2)}$	2.259	3.037(5)	149.49
N4−H4N···O1$^{(3)}$	2.348	2.949(6)	117.73
N4−H4N···O3$^{(4)}$	2.518	3.453(8)	155.64
O13−H80···O8	2.226	2.836(6)	131.40

[a] For atom numbering, see Figure 5; symmetry operations: (1) $x-1$, y, z; (2) $x+1$, y, z; (3) x, $y+1$, z; (4) $x-1$, $y+1$, z. [b] In Å. [c] In degrees.

And, therefore, the crystal packing is almost identical to that described for **1a** (see Figures S5−S6, Supporting Information) and needs no further comments.

A crystal suitable for single crystal X-ray diffraction studies could also be obtained from isopropanol. In this case, no solvent molecules are involved in the crystal structure of **1c**, probably due to the larger size of the isopropanol molecule, that can no longer be accommodated in the cavity between two molecules of **1** (Figure S7, Supporting Information). The peptide conformation is different from that in **1a** and **1b**. The torsion angle ψ of the D-Imz ring is 41.5° now in comparison to −163.2°/−150.8° and −165.5°/−151.7° for the two peptide molecules in the unit cells of **1a** and **1b**, respectively. This value corresponds to that observed for the D-Oxd moiety in the crystals of the peptide Boc-L-Phe-D-Oxd-OBn.[7] In the crystal packing of **1c**, two different types of intermolecular hydrogen bonds are present (Figure 7). One hydrogen bond connects the amidic NH hydrogen of the L-Phe unit with the carbonyl oxygen of the CO group of the D-Imz moiety belonging to another peptide molecule. The other involves the NH proton of the D-Imz ring and the carbonyl oxygen of a *t*-Boc group of another peptide molecule. These weak interactions generate also a 2D-network parallel to the *ab* plane, which is different from that observed in the packing of **1a** and **1b**, respectively (Tables 3 and 4). Quantum chemical calculations on the two different crystal packings with six peptide molecules but without solvent molecules show a slight preference for the packing of **1c** by 8.3 kJ/mol at the HF/6-31G* level of ab initio MO theory. By interaction with an additional solvent molecule, the methanol/ethanol solvate packings can obviously compensate for this disadvantage.

In order to investigate the effect of temperature on the structure of the plate-like crystals of **1a**, **1b**, and **1c**, calorimetric and X-ray powder diffraction analyses were carried out (Figure 8). The heating profile of single crystals of **1a** (Figure 8a) shows a broad endothermic peak at 46 °C followed by two sharp endothermic peaks, a strong one at 89 °C and a weak one at 141 °C. For a better understanding, the structural reorganization of **1a** associated with the thermal treatment was followed by X-ray powder diffraction (Figure 8b). The experimental X-ray diffraction pattern of **1a** collected at room temperature (Figure 8b, polymorph **1a-I**) shows all the peaks present in the diffraction pattern calculated from the single crystal structure of **1a** (Figure 8b, polymorph **1a-C**) and some additional peaks belonging to the diffraction pattern of **1a** after the thermal treatment just above the temperature first endothermic peak (Figure 8b, polymorph **1a-II**). The **1a** material TGA profile analysis indicates a weight loss of 3.8% in the temperature range between 23 and 68 °C (Figure S8, Supporting Information). Thus, the first endothermic peak

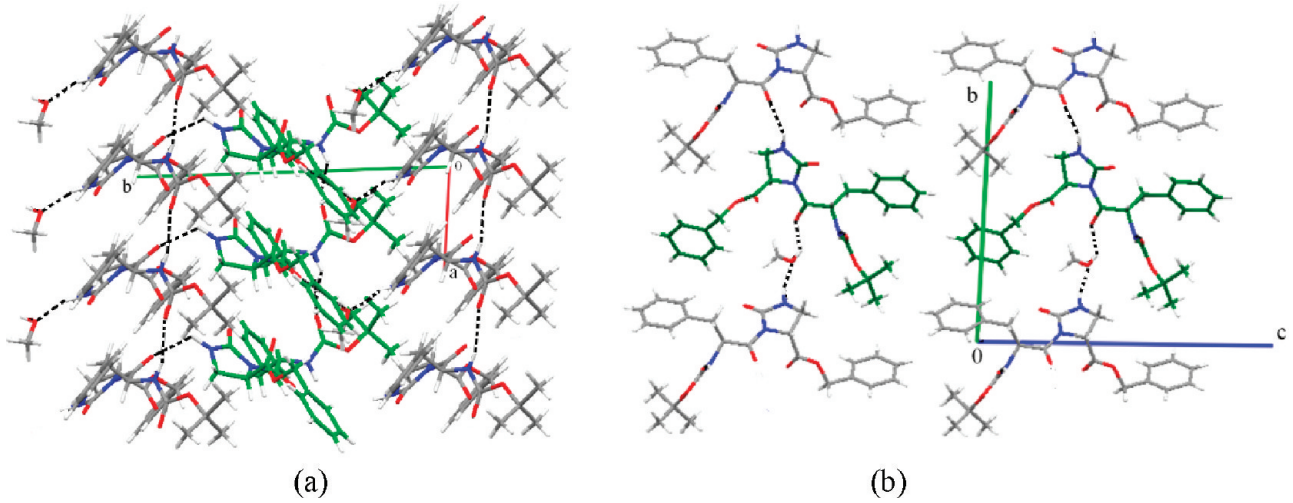

Figure 6. (a) View down the *c* axis showing the chains of the two different conformers running along the *a* axis; (b) view down the *a* axis showing the H-bond interactions among chains of the two different conformers of **1a**. Dark dotted lines indicate hydrogen bonds; color code: C gray (in one conformer) and green (in the second conformer), O red, N blue.

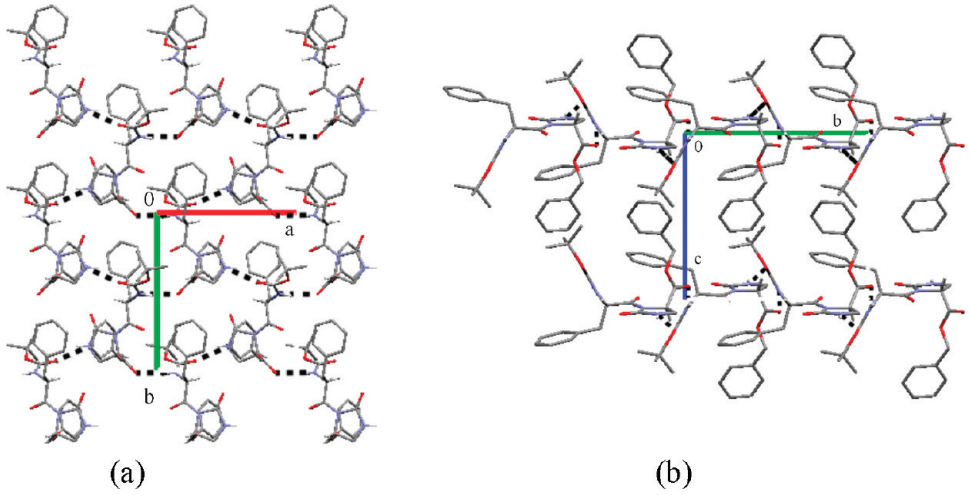

Figure 7. (a) View down the *c* axis and (b) view down the *a* axis of the crystal packing of **1c** (hydrogen atoms omitted for clarity).

Table 3. Backbone Torsion Angles in the Peptide Molecule of 1c

torsion angle[a]	deg
C22−N3−C14−C3 (ϕ1)	−108.5(1)
N3−C14−C3−N2 (ψ1)	158.7(1)
N2−C4−C6−O4 (ϕ2)	41.5(2)

[a] For atom numbering, see Figure 5.

Table 4. Hydrogen Bond Parameters for 1c[a]

D−H···A	H···A[b]	D···A[b]	∠D−H···Ac[c]
N3−H3N···O3$^{(1)}$	2.25(2)	3.072(1)	155(2)
N1−H1N···O5$^{(2)}$	2.14(2)	2.899(2)	148(2)

[a] For atom numbering, see Figure 5; symmetry operation: (1) $-x$, $y - 0.5$, $-z$. (2) $x + 1$, $y + 0.5$, $-z$. [b] In Å. [c] In degrees.

could be associated with the loss of methanol molecules from the crystal lattice (stoichiometric content of 3.3% w/w). These observations suggest that the material precipitating at room temperature is a mixture of crystals containing solvent and solvent-free crystals. No differences in the morphology of these two species of crystals have been observed. Above a temperature of 100 °C after the strong endothermic peak at 89 °C, the polymorph of **1a-III** is formed, which melts at a temperature of 141 °C giving an amorphous material (Figure 8b, polymorph **1a-IV**). The heating profile of single crystals of **1b** (Figure 8c) shows two overlapping endothermic peaks at 95 and 109 °C followed by a very weak one at 144 °C.

Also in this case the structural reorganization of **1b** associated with the thermal treatment was followed by X-ray powder diffraction (Figure 8d). The experimental X-ray diffraction pattern of **1b-I** collected at room temperature shows all the peaks present in the diffraction pattern calculated from the single crystal structure of **1b-C**. This indicates that the material precipitating at room temperature is a pure phase. At a temperature of 97 °C after the endothermic peak at 95 °C, a second polymorph of **1b-II** is formed. This polymorph melts at a temperature of 109 °C giving the amorphous material **1b-III**. The material **1b** TGA profile indicates a weight loss of 5.8% in the range of temperature between 65 and 120 °C (Figure S8, Supporting Information). This value is close to the stoichiometric content of solvent in **1b** (5.8% *w*/*w*).

Finally, single crystals of **1c** (Figure 8e) show a heating profile, in which only one strong endothermic peak at 150 °C

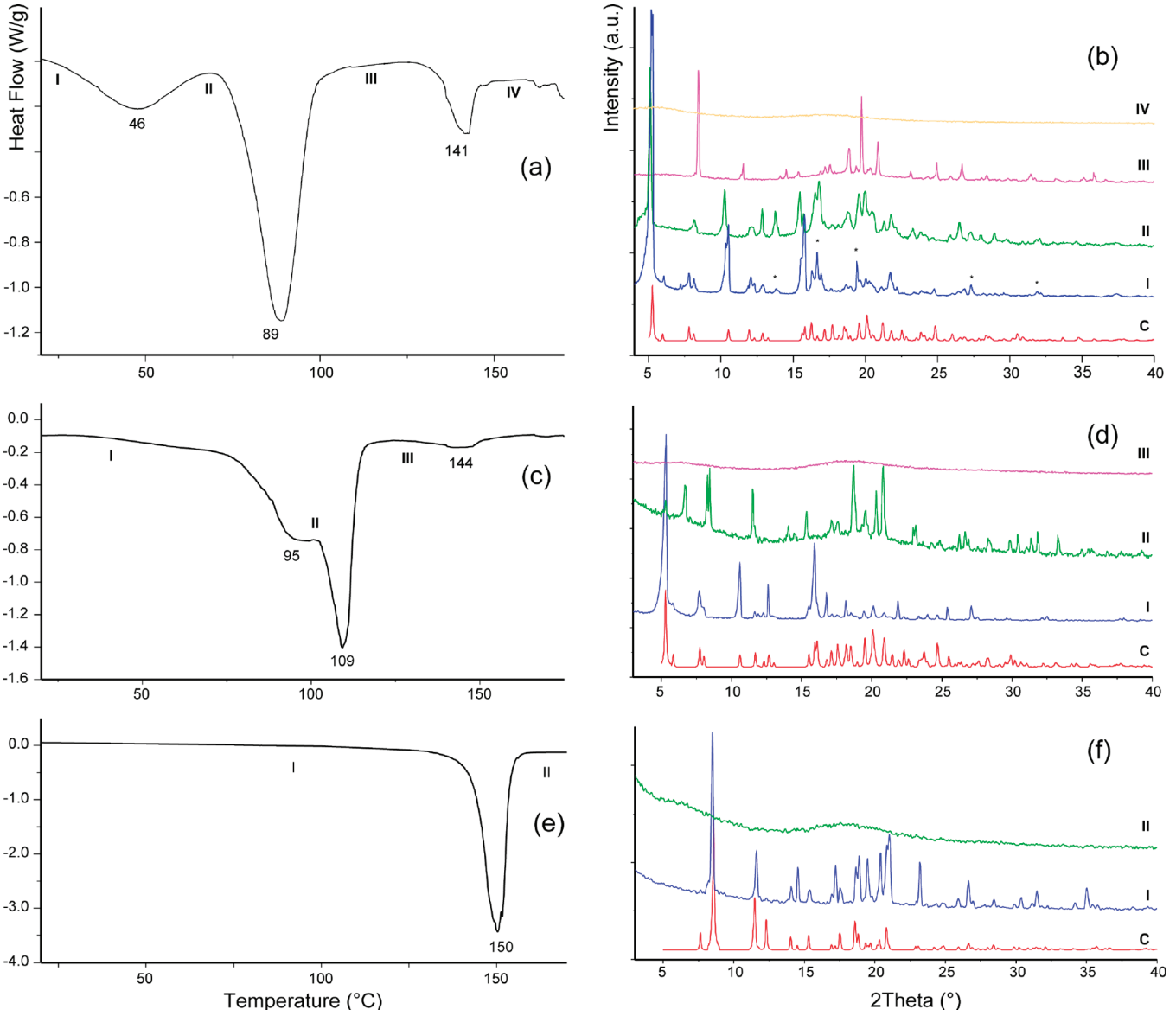

Figure 8. Differential scanning calorimetry profiles of crystals of **1** precipitated from a solution of (a) methanol (**1a**), (c) ethanol (**1b**), and (e) isopropanol (**1c**). (b) X-ray powder diffraction patterns of single crystals of **1a** after thermal treatment up to the temperature I−IV. (d) X-ray powder diffraction patterns of single crystals of **1b** after thermal treatment up to the temperature I−III. (f) X-ray powder diffraction patterns of single crystals of **1c** after thermal treatment up to the temperature I and II. In panels b, d, and f, the calculated powder diffraction pattern from the single crystal structure (c) is reported for comparison with I. In panel b, the asterisks in I indicate the diffraction peaks, which belong to the desolvated form II.

is present. The material **1c** is a pure phase, as shown by the correspondence among all the peaks present in the experimental X-ray powder diffraction pattern (Figure 8f, **1c-I**) and the one calculated from the single crystal structure (**1c-C**). Moreover, this compound melts at 150 °C, giving the amorphous material **1c-II**. This material does not host solvent in its crystal lattice, as confirmed by the absence of peaks in the first derivative of the TGA profile below the decomposition temperature (Figure S8, Supporting Information). All these materials start to decompose at temperatures above 180 °C (see TGA profiles in Figure S8, Supporting Information).

Conclusions

The pseudopeptide Boc-L-Phe-D-Imz-OBn **1** has been designed and prepared to obtain a molecule, able to form cross-linked hydrogen bonds. Crystallization of this compound from methanol and ethanol provides solvate structures **1a** and **1b** with similar unit cell parameters. In both cases, the peptide crystallizes in infinite chains with the peptide monomers in a parallel arrangement connected by a single hydrogen bond. The chains are in antiparallel orientation and cross-linked by hydrogen bonds employing the heterocyclic NH group of the D-Imz ring. Thus, a 2D network made of layers parallel to the *ab* plane results producing a plywood structure. Crystallization of the peptide from isopropanol provides also a 2D network by hydrogen bond cross-linking. However, this network does not involve solvent molecules and has a structure completely different from the networks crystallizing with methanol and ethanol. The degree of order in crystal assembly is continuously decreasing from methanol to ethanol and isopropanol.

Acknowledgment. G.A., S.C., G.F., M.M., and C.T. are grateful to Ministero dell'Università e della Ricerca Scientifica

(PRIN 2006), Università di Bologna (Funds for selected topics), and Fondazione del Monte di Bologna e di Ravenna for financial support. H.-J.H. thanks Deutsche Forschungsgemeinschaft (SFB 610, HO 2346/1-3) for funding.

Supporting Information Available: Crystallographic data (cif files) for **1a**, **1b** and **1c**. Supplemental crystallographic Figures of **1a**, **1b** and **1c**. This material is available free of charge via the Internet at http://pubs.acs.org.

References

(1) (a) Gellman, S. H. *Acc. Chem. Res.* **1998**, *31*, 173–180. (b) Hill, D. J.; Mio, M. J.; Prince, R. B.; Hughes, T. S.; Moore, J. S. *Chem. Rev.* **2001**, *101*, 3893–4011. (c) Cheng, R. P.; Gellman, S. H.; DeGrado, W. F. *Chem. Rev.* **2001**, *101*, 3219–3232.

(2) (a) Huc, I. *Eur. J. Org. Chem.* **2004**, 17–29. (b) Hecht, S.; Huc, I., Eds.; *Foldamers: Structure, Properties, and Applications*; Wiley-VCH: Weinheim, Germany, 2007.

(3) (a) Lai, X.-Z.; Feng, Y.; Pollard, J.; Chin, J. N.; Rybak, M. J.; Bucki, R.; Epand, R. F.; Epand, R. M.; Savage, P. B. *Acc. Chem. Res.* **2008**, *41*, 1233–1240. (b) Tsantrizos, Y. S. *Acc. Chem. Res.* **2008**, *41*, 1252–1263. (c) Sun, H.; Nikolovska-Coleska, Z.; Yang, C.-Y.; Qian, D.; Lu, J.; Qiu, S.; Bai, L.; Peng, Y.; Cai, Q.; Wang, S. *Acc. Chem. Res.* **2008**, *41*, 1264–1277. (d) Robinson, J. A. *Acc. Chem. Res.* **2008**, *41*, 1278–1288.

(4) (a) Takahashi, T.; Mihara, H. *Acc. Chem. Res.* **2008**, *41*, 1309–1318. (b) Sato, J.; Takahashi, T.; Oshima, H.; Matsumara, S.; Mihara, H. *Chem.—Eur. J.* **2007**, *13*, 7745–7752. (c) Mishra, R.; Bulic, B.; Sellin, D.; Jha, S.; Waldmann, H.; Winter, R. *Angew. Chem., Int. Ed.* **2008**, *47*, 4679–4682.

(5) Sakamoto, J.; van Heijst, J.; Lukin, O.; Schlüter, A. D. *Angew. Chem., Int. Ed.* **2009**, *48*, 1030–1069.

(6) Ulijn, R. V.; Smith, A. M. *Chem. Soc. Rev.* **2008**, *37*, 664–675.

(7) Angelici, G.; Falini, G.; Hofmann, H.-J.; Huster, D.; Monari, M.; Tomasini, C. *Angew. Chem., Int. Ed.* **2008**, *47*, 8075–8078.

(8) Guha, S.; Drew, M. G. B.; Banerjee, A. *CrystEngComm* **2009**, DOI: 10.1039/b814454k.

(9) *SMART & SAINT Software Reference Manuals, version 5.051* (*Windows NT Version*); Bruker Analytical X-ray Instruments Inc.: Madison, WI, 1998.

(10) Sheldrick, G. M. *SADABS, Program for Empirical Absorption Correction*; University of Göttingen: Göttingen, Germany, 1996.

(11) Altomare, A.; Burla, M. C.; Camalli, M.; Cascarano, G. L.; Giacovazzo, C.; Guagliardi, A.; Moliterni, A. G. G.; Polidori, G.; Spagna, R. *J. Appl. Crystallogr.* **1999**, *32*, 115–119.

(12) Sheldrick, G. M. *SHELXTLplus Version 5.1* (*Windows NT version*)-*Structure Determination Package*; Bruker Analytical X-ray Instruments Inc.: Madison, WI, 1998.

(13) Frisch, M. J. et al. *Gaussian 03, Revision C.02*; Gaussian Inc.: Wallingford CT, 2004.

(14) Angelici, G.; Contaldi, S.; Green, S. L.; Tomasini, C. *Org. Biomol. Chem.* **2008**, *6*, 1849–1852.